Investigation of the Coordination State of Aluminum in β Zeolites by X-ray Photoelectron Spectroscopy

F. Collignon,[†] P. A. Jacobs,[†] P. Grobet,[†] and G. Poncelet*,[‡]

Unité de Catalyse et Chimie des Matériaux Divisés, Université Catholique de Louvain, Place Croix du Sud 2/17, B-1348 Louvain-la-Neuve, Belgium, and Centrum voor Oppervlaktechemie en Katalyse, Katholieke Universiteit Leuven, Kasteelpark, Arenberg 21, B-3001, Leuven, Belgium

Received: February 16, 2001; In Final Form: May 3, 2001

β zeolites have been characterized by X-ray photoelectron spectroscopy (XPS). Owing to the small crystallite size (20 nm), nearly 90% of the Si and Al content can be estimated from the Si 2p and Al 2p peaks. The chemical state of Al was established by decomposition of the Al KLL Auger transition. Three types of Al could be differentiated: tetrahedral (Al^{IV}), octahedral (Al^{VI}), and tricoordinated (Al^{III}). From the decomposition of the Al KLL peak of a β zeolite calcined to remove its template, it was found that Al^{IV} transforms to Al^{III} and Al^{VI}. Reversibility of Al^{III} to Al^{IV} also occurred when the sample was ammonium-exchanged, confirming ^{27}Al MAS NMR results.

Introduction

The catalytic activity of a zeolite depends not only on its aluminum content but also on the coordination state of aluminum. Several authors investigated the stability of the tetrahedral aluminum sites in β zeolite by ^{27}Al MAS NMR spectroscopy.[1−4] These studies have shown the presence of two kinds of Al: framework Al in 4-fold coordination (with signal at 54 ppm) and Al in 6-fold coordination (signal at 0 ppm). No signal at 30 ppm characteristic of pentacoordinated or distorted tetrahedral Al, commonly found in dealuminated Y zeolites and mordenites, was observed in the spectra. The $Al^{IV}-Al^{VI}$ interconversion in β zeolites appears to be reversible under mild treatment such as cation exchange (K^+)[1,2] and NH_3 adsorption[2] or in the presence of H_2O produced in methanol dehydration.[4] Reversible tetrahedral−octahedral Al interconversion in Y zeolites has been recently reported.[5]

The "bridging hydroxyl" formed by protons compensating for the excess negative charges constitute the "classical" Brønsted acid sites present in zeolites. In β zeolite, these OH groups give rise to an IR band showing up at 3610 cm^{-1}.[1−3,6−9] Two other types of Brønsted acid sites, with IR bands at 3660 and 3780 cm^{-1}, have been observed upon calcination of β zeolite in deep-bed conditions or at temperatures higher than 500 °C.[7] The AlO−H groups giving rise to a vibration at 3660 cm^{-1} have been assigned to extraframework silica−alumina Al−OH groups[6] or to Al−OH groups partially connected to the zeolite framework.[10] The AlO−H species related to the "very high frequency" (VHF) band at 3780 cm^{-1}, with higher acid strength than the silanol groups,[6] have been recently associated with tricoordinated aluminum atoms linked to two oxygen atoms of the zeolite framework.[6,11] Vimont et al.[11] proposed to assign those sites to Lewis acid sites. The presence of tricoordinated Al has already been observed in dealuminated mordenites by the decomposition of the XPS-Al KLL peak.[12,13] In contrast to MAS NMR spectroscopy where part of the Al (invisible Al) is not detected, all the aluminum atoms present at the outer surface are analyzed with the XPS technique.

In this study, different β zeolites have been investigated with X-ray photoelectron spectroscopy with the aim of examining the different coordination states of aluminum and the possible presence of tricoordinated Al. Owing to the small crystallite size of these zeolites (20 nm), nearly 90% of the atoms are detected by this technique, which probes a depth between 2 and 10 nm.

Experimental Section

Zeolites. The β zeolites considered in this study and their Si/Al ratio are indicated in Table 1. ZB25 and ZB25T were commercial samples from PQ Zeolite, ZB25T being an as-synthesized β still containing Na^+ and its template (tetraethylammonium).

Sample ZB25 (in the protonic form) was acid dealuminated following the method of Fajula et al.:[14] 1 g of zeolite was added to 200 mL of 0.02−0.09 M solutions of HNO_3 previously heated at 80 °C, and the mixture was stirred for 3 h at that temperature. The solids were washed and dried for 1 h at 100 °C.

Elimination of the template of ZB25T was achieved by temperature-programmed calcination in flowing N_2 between room temperature and 120 °C, with a plateau for 1 h, and from 120 to 540 °C, using a ramp of 5 °C min^{-1}. At 540 °C, nitrogen was switched for oxygen, and the treatment was maintained for 3.5 h (sample ZB25T c(3.5)) or 13 h (ZB25T c(13)).

The NH_4^+ form of ZB25T c(13) was prepared by adding 1 g of zeolite to 200 mL of 2 M solution of ammonium acetate heated at 80 °C and stirring overnight. After filtration and washing (followed by conductivity measurements), the sample was dried at 60 °C for 1 h. Conversion of the ammonium (ZB25T c(13)-e) to the H-form (ZB25T c(13)-e−c) was done under flowing air using the same heating rate as above, except that the final temperature (500 °C) was maintained for 10−15 h.

In addition to the commercial samples, β zeolites were synthesized following a procedure similar to that of Borade and Clearfield[15] in the presence of tetraethylammonium hydroxide as template. TEAOH (35 wt % aqueous solution, from Aldrich) was mixed in deionized water with sodium aluminate (37 wt

[†] Katholieke Universiteit Leuven.
[‡] Université Catholique de Louvain.

10.1021/jp0106202 CCC: $20.00
Published on Web 06/22/2001

TABLE 1: Si/Al (Bulk) Ratio, Relative Crystallinity (%), External Surface Area (S_{ext}, $m^2\ g^{-1}$), and Micropore Volume (V_μ, $cm^3\ g^{-1}$)

zeolite	Si/Al[a]	rel cryst	S_{ext}[b]	V_μ[b]
ZB25	13.4	100	241	0.16
ZB25 0.02	17.7	94	n.d.	n.d.
ZB25 0.03	18.1	94	255	0.18
ZB25 0.05	21.3	91	252	0.16
ZB25 0.06	21.9	98	n.d.	n.d.
ZB25 0.09	28.5	91	263	0.18
ZB25T	11.8	157	n.d.	n.d.
ZB25T c(3.5)	11.8	82	233	0.19
ZB25T c(13)	11.8	95	n.d.	n.d.
ZB25T c(13)-e	n.d.	n.d.	n.d.	n.d.
ZB25T c(13)-e-c	n.d.	80	n.d.	n.d.
ZBL18T c	9.2	90	188	0.19
ZBL28T c	14.6	102	278	0.21
ZBL36T c	17.9	95	167	0.16

[a] From ICPS. [b] Calculated according to ref 16. [c] n.d.: not determined.

% Na_2O, 56 wt % Al_2O_3, from Carlo Erba) in a Teflon cylinder and stirred for 10 min. Silica (Degussa FK300DS) was progressively supplied to the solution. The SiO_2/TEAOH and H_2O/SiO_2 molar ratios were 6 and 6.1, respectively. The Si/Al molar ratio of the "dry" mixture was changed by adjusting the amount of sodium aluminate. The powder was mixed at 60−70 rpm for 30−40 min until a thick slurry was obtained. Crystallization was carried out in a nonstirred Parr pressure vessel (using Teflon cylinders) heated for 48 h at 170 °C. The solid was washed by filtration with hot deionized water (25 mL/g of solid), and dried at 60 °C. Zeolites with Si/Al ratios of 9.2, 14.6, and 17.9 were synthesized (samples ZBL in Table 1). They were calcined for 3.5 h in order to eliminate the template (samples ZBL c) under the conditions indicated above.

Characterization. The bulk Si/Al ratios were established from the Al contents obtained by inductively coupled plasma spectroscopy (ICPS). The relative crystallinity of the samples was evaluated from the X-ray diffraction patterns recorded with a Kristalloflex D-5000 (Siemens) equipment (monochromated Cu Kα radiation), relating the area of the [302] reflection at 22.43° 2θ to that of sample ZB25.

The textural characteristics were obtained from nitrogen adsorption−desorption isotherms recorded at liquid nitrogen temperature with an ASAP 2000 sorptometer (Micromeritics), using the "t-plot" approach[16] for the determination of the external surface areas (S_{ext}) and micropore volumes (V_μ), with the linear regression being made in the range $0.35 < t < 0.5$ nm.

The XPS analyses were performed with a Vacuum Generators ESCA 3MK II spectrometer equipped with a Tracor Northern TN 1710 signal averager. The residual pressure in the analysis chamber was lower than 10^{-6} Pa. The (nonmonochromated) X-ray source was generated by a Mg anode ($h\nu = 1253.6$ eV) powered at 14 kV and with an emission current of 20 mA. The constant pass energy in the hemispherical analyzer of 50 eV and the slit width of 4 mm gave an energy resolution of 2.0 eV, expressed by the full width at half-maximum (fwhm) of Au $4f_{7/2}$. The energy scale of the spectrometer was calibrated with the Au $4f_{7/2}$ binding energy fixed at 84.0 eV. Photoelectron detection was made at an angle of 45° to the sample normal.

The powdered sample was pressed in a stainless steel sample holder (8 mm diameter) by means of a polyacetal (Delrin) cylinder, following the procedure of Rouxhet and Genet.[17] Charge correction was made by fixing the binding energy of the C-(C, H) component of the C 1s peak of adventitious carbon at 284.8 eV. The peaks were decomposed using a least-squares fitting routine (ESCA 8.3 D software from Interface Science Instruments) with a Gauss/Lorenz ratio of 70/30 and after subtraction of a linear background. The atomic concentration ratios were calculated from the peak areas normalized on the basis of acquisition parameters and sensitivity factors of Wagner et al.[18] (0.28, 0.185, 2.3, and 0.42 for Si 2p, Al 2p, Na 1s, and N 1s, respectively). This can be done because the analyzer transmission function varies with the inverse of the photoelectron kinetic energy, as required by Wagner's data. Before XPS analysis, it was controlled that the Mg anode was not contaminated with Al, to verify that no Si 2p peak generated by the X-ray of the Al anode interfered with the Al KLL peak induced by the Bremsstrahlung radiation of the nonmonochromatized magnesium X-ray source.[13]

Results and Discussion

The Si/Al bulk ratios, relative crystallinities, micropore volumes (V_μ) and external surface areas (S_{ext}) of the different zeolites are indicated in Table 1. Dealumination of ZB25 by acid leaching affected both the bulk Si/Al ratio and the relative crystallinity (samples ZB25 0.02 to 0.09). The noncalcined β zeolite containing the template (ZB25T) showed the highest crystallinity. The crystallinity of the calcined forms (ZB25T c(3.5) and -c(13)) was similar to that of ZB25. The lab-synthesized samples (ZBL T) and ZB25 showed equivalent crystallinity. All the β zeolites developed a rather large external surface area (between 167 and 278 $m^2\ g^{-1}$) and micropore volumes in the range 0.16−0.21 $cm^3\ g^{-1}$.

The Si/Al atomic ratios obtained by XPS, the binding energy (BE, eV), and the full width at half-maximum (fwhm, in eV) of the Si 2p and Al 2p peaks are given in Table 2. The XPS Si/Al atomic ratios were close to those obtained by ICPS (Table 1), as shown by the good relationship of Figure 1 (slope: 1.137 ± 0.058; intercept: 1.691 ± 1.027), indicating that bulk and surface chemical compositions were nearly identical, owing to the small crystallite size of β zeolite.

Coutanceau et al.[19] observed by TE microscopy that the crystals of ZB25 (0.1−0.7 μm) consisted of the agglomeration of crystallites smaller than 20 nm. An estimation of the crystallite diameter (nm) of the β zeolite was done, assuming a framework density (FDz) of 15.6 tetrahedra/nm^3 and that S_{ext} is a measure of the mesoporous surface area generated by the outer surface of the crystallites (in $m^2\ g^{-1}$) using the following formula:

$$d = 6 \times 10^{-18} N(\mathrm{FDz}60S_{ext})^{-1}$$

where N is the Avogadro number. A value of 20 nm was obtained for an average surface area of 200 $m^2\ g^{-1}$. The analysis depth can be estimated from Z (depth) $= 3\lambda \cos 45°$, where λ is the electron inelastic mean free path. In SiO_2, $\lambda_{Si} = 2.6$ nm, whereas in alumina, λ_{Al} values between 1.9 and 2.4 nm have been reported (according to the authors).[20] Using an average value of $\lambda = 2.5$, an analysis depth of about 5.3 nm is obtained. Since 95% of the signal is coming from a depth of about 5 nm (half the crystallite radius), one may estimate that nearly 87.5% of the crystallite volume of the zeolite was explored by the XPS technique.

The BE of Si 2p and Al 2p levels varied between 102.7 and 104.1 eV and between 73.9 and 75.2 eV, respectively. These values are close to those obtained by Borade and Clearfield[21] for β and H−Y zeolites, and by Remy et al. for mordenites[12] and US−Y.[13] Curiously, the ammonium-exchanged zeolite

TABLE 2: Si/Al XPS Atomic Ratio, Binding Energies (BE, eV), and Full Widths at Half-Maximum (FWHM, eV) of Si 2p and Al 2p Peaks and Kinetic Energy (eV), FWHM (eV), and Modified Auger Parameter (α', eV) of the Al KLL Peak

		Si 2p		Al 2p		Al KLL		
zeolite	Si/Al	BE	FWHM	BE	FWHM	KE	FWHM	α′ [a]
ZB25	12.5	103.8	2.7	75.0	3.1	1385.1	3.6	1460.1
ZB25 0.02	17.5	103.4	2.7	74.7	2.9	1385.4	3.5	1460.1
ZB25 0.03	19.1	103.7	2.8	75.0	3.0	1385.3	3.5	1460.3
ZB25 0.05	22.0	103.5	2.7	74.5	2.9	1385.8	3.3	1460.3
ZB25 0.06	23.6	103.5	2.6	75.3	3.0	1384.8	3.7	1460.1
ZB25 0.09	31.5	103.5	2.6	74.5	3.0	1385.3	4.2	1459.8
ZB25T	10.8	103.1	2.4	74.0	2.3	1386.5	2.6	1460.5
ZB25T c(3.5h)	13.6	103.4	2.4	74.7	2.7	1385.8	3.1	1460.5
ZB25T c(13h)	13.9	103.5	2.4	74.7	2.7	1385.8	3.2	1460.5
ZB25T c(13h)-e	10.7	102.7	2.5	73.9	2.6	1386.5	2.9	1460.4
ZB25T c(13h)-e-c	14.0	103.7	2.6	75.2	3.0	1385.2	3.3	1460.4
ZBL18T c	9.9	103.8	2.4	75.1	2.8	1385.3	3.0	1460.4
ZBL28T c	14.0	103.6	2.5	74.9	2.9	1385.3	3.0	1460.2
ZBL36T c	18.9	104.1	2.5	75.2	3.1	1385.6	3.2	1460.8

[a] α′ = BE Al 2p + KE Al KLL.

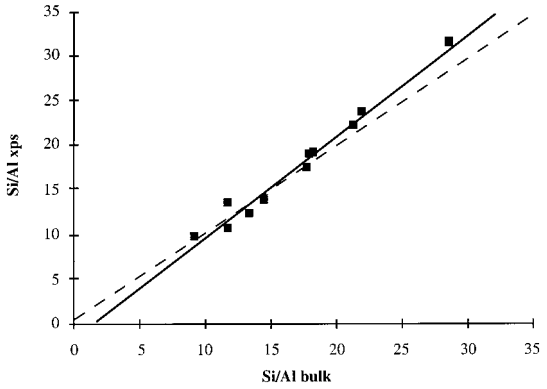

Figure 1. Relation between "surface" and bulk Si/Al atomic ratio for the different β zeolites.

(ZB25T c(13)-e) showed the lowest BE values for Si 2p (102.7 eV) and Al 2p (73.9 eV).

Vaudry et al.[22] showed that for an as-synthesized β zeolite with Si/Al molar ratio higher than 10.8, all the template molecules were associated with framework Al, the Na cations being located at structural defects (SiONa). The N/Al XPS atomic ratios of samples ZB25T and ZB25T c(13)-e, which contained nitrogen were 1.00 and 0.82, respectively. It may thus be admitted that all the aluminum atoms in ZB25T occupied framework positions, namely, with 4-fold coordination.

As the photoionization process leaves both an ion in an excited state and an electron vacancy at a lower level, relaxation takes place via either X-ray emission or the "Auger effect". The relaxation process responsible for the Auger peak of aluminum atoms involves one electron vacancy in the K (1s) shell generated by the Bremsstrahlung of the nonmonochromatized X-ray source, and two electrons of the L (2s, or 2p) shell. One of the L electrons is ejected from the Al atom, while the other one jumps on the K level.

The sum of the binding energy of the Al 2p photoelectron (BE Al 2p) and the kinetic energy of the photoelectron resulting from the Al KLL peak (Table 2) provides the modified Auger parameter (α′). This parameter is independent of the X-ray excitation energy and charge effect[23] and is related, in the case of aluminosilicates, to the polarizability of the near neighboring oxygen atoms.[24]

The values of the modified Auger parameter (α′ in Table 2) were in the range 1459.8−1460.8 eV, typical of aluminum in 4-fold coordination for the samples used in this study. ZB25T, still containing its template, had a fwhm of the Si 2p peak slightly superior to that of Al 2p and had the smallest fwhm of the Al KLL peak. Its α′ value close to 1460 eV led us to consider the aluminum to be mainly in 4-fold coordination (Al^{IV}).[25] The larger fwhm values for the other samples reasonably allowed us to suspect the existence of other coordination state(s). For example, quantitative ^{27}Al MAS NMR analysis of sample ZB25 showed the presence of 58% Al^{IV} (signal at 54 ppm) and 25% Al^{VI} (0 ppm), the difference (17%) obtained by subtracting the Al content established by quantitative ^{27}Al MAS NMR from that determined by ICPS, representing the "invisible" Al.

Dealumination of ZB25 by acid leaching resulted in a decrease of the fwhm of the Al KLL peak for the most diluted solutions, and an increase for solutions with higher concentrations (Table 2). The decreasing fwhm values (up to 0.05 M) are associated with the partial elimination of extraframework Al (42% as established by ^{27}Al MAS NMR), which acts as a poison to the acid sites.[9,19] These samples adsorbed higher amounts of ammonia and were more active in the synthesis of ethyl *tert*-butyl ether than ZB25.[26] A similar effect was also observed upon calcination of the template-containing ZB25T, with longer calcination time increasing the fwhm of the Al KLL peak. Interestingly, ammonium exchange of ZB25T c(13) brought about a decrease of its fwhm (ZB25T c(13)-e in Table 2). Subsequent deammoniation of ZB25T c(13)-e resulted in an increase of the fwhm from 2.9 to 3.3 eV. This increase suggests the existence of tetrahedral−octahedral aluminum reversibility, consistently with ^{27}Al MAS NMR results.[1−5]

Decomposition of Al KLL Peak. For ZB25T with a bulk Si/Al ratio of 11.8, the $(N/Al)_{xps}$ atomic ratio of 1, on one hand, and the fwhm (Al 2p)/fwhm (Si 2p) ratio lower than unity, on the other hand, constitute a strong presumption that all the aluminum atoms are in 4-fold coordination.[22,25] The small fwhm value of its Al KLL peak (2.6 eV) is close to that found under similar experimental conditions for pyrophyllite (2.8 eV) containing only octahedral Al.[12] For these reasons, ZB25T could reasonably be used as a standard for the decomposition of the Al KLL peak. For the other β zeolites, decomposition was done because their Al KLL peaks were broader than that of ZB25T (Table 2).

All the Al KLL peaks exhibited a symmetrical shape. The absence of inflection could lead to meaningless decompositions. To minimize the number of solutions, a fwhm of 2.7 eV (mean value of 2.6 and 2.8 eV) was imposed. Table 3 compiles the kinetic energy values obtained from the decomposition the Al KLL peaks with two and three components, whereas the

TABLE 3: χ^2, Kinetic Energies (eV), and Fractions from the Decomposition of the Al KLL Peak with Two or Three Components

	decomposition with two components					decomposition with three components						
		component I		component II			component I		component II		component III	
zeolite	χ^2	KE	%	KE	%	χ^2	KE	%	KE	%	KE	%
ZB25	5.8	1384.6	70	1386.3	30	5.1	1383.1	11	1384.8	62	1386.3	27
ZB25 0.02	9.5	1385.8	68	1384.2	32	9.2	1383.1	13	1385.2	61	1386.5	26
ZB25 0.03	4.6	1385.7	71	1383.9	29	4.4	1383.4	16	1385.2	64	1386.6	20
ZB25 0.05	5.9	1385.9	83	1383.6	17	5.9	1383.5	15	1385.7	73	1386.8	12
ZB25 0.06	6.7	1385.2	60	1383.6	40	6.7	1383.7	36	1385.1	59	1386.1	5
ZB25 0.09	7.8	1385.8	66	1383.7	34	7.6	1383.9	37	1385.6	43	1386.7	20
ZB25T		1386.5	100						1386.5	100		
ZB25T c(3.5h)	7.2	1386.0	82	1384.5	18	6.8	1384.5	15	1386.0	83	1386.7	2
ZB25T c(13h)	4.9	1386.0	66	1385.1	34	4.4	1384.3	14	1385.8	77	1386.7	9
ZB25T c(13h)-e	4.0	1386.3	82	1387.2	18	4.6	1384.4	6	1386.4	84	1387.2	10
ZB25T c(13h)-e-c	5.5	1384.4	59	1383.0	41	5.3	1382.6	17	1384.0	73	1386.2	10
ZBL18T c	9.7	1385.7	70	1384.5	30	9.8	1383.9	13	1385.5	85	1386.3	2
ZBL28T c	4.9	1385.4	83	1386.8	17	4.9	1383.6	10	1385.4	82	1386.8	8
ZBL36T c	6.0	1385.3	79	1386.9	21	5.6	1383.4	5	1385.4	77	1387.0	18

TABLE 4: Modified Auger Parameter (α' Al KLL, eV) from the Sum of the BE of Al 2p and the KE of the Components Obtained after Decomposition of the Al KLL Peak

	two components		three components		
zeolite	Al^{IV} (α')	$Al \neq Al^{IV}$ (α')	Al^{III} (α')	Al^{IV} (α')	Al^{VI} (α')
ZB25	1459.6	1461.3	1458.1	1459.8	1461.3
ZB25 0.02	1460.5	1458.9	1457.8	1459.9	1461.2
ZB25 0.03	1460.7	1458.9	1458.4	1460.2	1461.6
ZB25 0.05	1460.4	1458.1	1458.0	1460.2	1461.3
ZB25 0.06	1460.5	1458.9	1459.0	1460.4	1461.4
ZB25 0.09	1460.3	1458.2	1458.4	1460.1	1461.2
ZB25T	1460.5			1460.5	
ZB25T c(3.5h)	1460.7	1459.2	1459.2	1460.7	1461.4
ZB25T c(13h)	1460.7	1459.8	1459.0	1460.5	1461.4
ZB25T c(13h)-e	1460.2	1461.1	1458.3	1460.3	1461.1
ZB25T c(13h)-e-c	1459.6	1458.2	1457.8	1459.2	1461.4
ZBL18T c	1460.8	1459.6	1459.0	1460.6	1461.4
ZBL28T c	1460.3	1461.7	1458.5	1460.3	1461.7
ZBL36T c	1460.5	1462.1	1458.6	1460.6	1462.2
mean	1460.4 ± 0.4	1459.7 ± 1.4	1458.5 ± 0.5	1460.2 ± 0.4	1461.4 ± 0.3

corresponding modified Auger parameters (α') are given in Table 4. Decomposition with two components resulted in average α' values of 1460.4 ± 0.4 and 1459.7 ± 1.4 eV. The first component could be attributed to tetrahedral aluminum, whereas the interval of incertitude of the second one (±1.4 eV) did not allow any allocation. When the curves were fitted with three components, the following average α' values were obtained: 1458.5 ± 0.5, 1460.2 ± 0.4, and 1461.4 ± 0.3 eV. For dealuminated mordenites, α' values in the ranges 1458.7−1459.3, 1459.8−1460.2, and 1460.9−1461.5 eV were attributed to Al^{III}, Al^{IV}, and Al^{VI}, respectively.[12] The α' values obtained for the β zeolites were included in those ranges and may thus be assigned to the three different types of Al. Also, the comparison of χ^2 (Table 3) showed that the experimental peak envelopes were generally better fitted when imposing three components instead of two. The decomposition of the Al KLL peak with three components for ZB25 is illustrated in Figure 2.

To assess the validity of the decomposition in three components, the percentage of Al^{IV} (component II) has been plotted against the fwhm of the Al KLL peak (Figure 3). The values obtained from the N/Al atomic ratios of ZB25T (100% Al^{IV}), and ZB25T c(13)-e (NH_4^+-exchanged, 82% Al^{IV}) have been included (full squares). The full circle represents the ratio 100-[Al^{IV}/(Al^{IV} + Al^{VI} + Al^{inv})] found independently by quantitative ^{27}Al MAS NMR and chemical analysis of Al of ZB25. The linear relationship supports the validity of the decomposition of the Al KLL peak with three components (imposing a fwhm value of 2.7 eV).

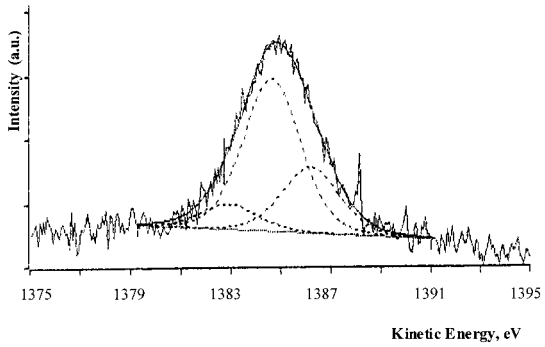

Figure 2. Decomposition of the Al KLL peak in three components for ZB25.

As in the case of dealuminated mordenites,[12] tricoordinated aluminum (Al^{III}) as well appears to exist in β zeolite, supporting the attribution by Vimont et al.[11] of the VHF IR band at 3780 cm^{-1} to an OH−Al^{III} species where the Al^{III} atom is connected to two oxygen atoms of the zeolite framework.

Effect of Calcination and Exchange on the Al Chemical State of Sample ZB25T. As mentioned earlier, the duration of the calcination and the exchange with ammonium had an influence on the FWMH of the Al KLL peak. Figure 3 showed that the variation of the fwhm was related to the variation of the Al^{IV} content of the zeolite: the larger the fwhm of the Auger peak, the lower the Al^{IV} content.

The percentage of Al^{IV} estimated from the decomposition of the Al KLL peak with three components has been plotted for

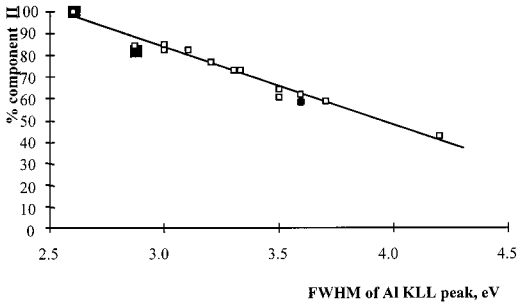

Figure 3. Percentage of Al^{IV} obtained with three components (□), $(N/Al\ 100)_{XPS}$ ratio of ZB25T and ZB25T c(13)-e (■), and $[Al^{IV}/(Al^{IV} + Al^{VI} + Al_{inv}) \times 100]_{NMR}$ of B25 (●) vs fwhm of the Al KLL peak obtained without decomposition.

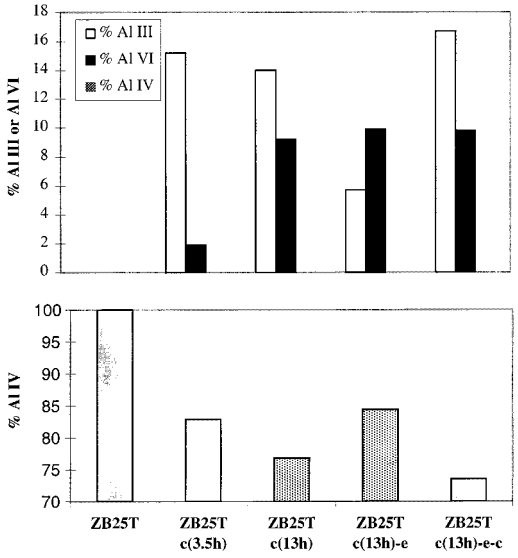

Figure 4. Percentages of Al^{IV}, Al^{III}, and Al^{VI} obtained with three components for ZB25T, ZB25T c(3.5), ZB25T c(13), ZB25T c(13)-e, and ZB25T c(13)-e−c.

the different samples of ZB25T (namely, ZB25T, -c(3.5), -c(13), -(13)-e, and -c(13)-e-c) in Figure 4. Calcination of ZB25T for 3.5 and 13 h decreased the fraction of tetrahedral Al, with a lower Al^{IV} content for the longer time. It is inferred from Table 3 that (ir)reversible transformation of framework Al^{IV} to extraframework Al^{VI} occurred for a calcination time between 3.5 and 13 h. An ammonium exchange of ZB25T c(13) increased the proportion of Al^{IV}. When sample ZB25T c(13)-e was calcined in order to convert it to the protonated form (ZB25T c(13)-e-c), the percentage of Al^{IV} again decreased. This phenomenon is consistent with the existence of a reversible aluminum, as found by other authors by ^{27}Al MAS NMR spectroscopy.[1−5] The results of Tables 3 and 4 and Figure 4 strongly suggest that tricoordinated aluminum would be responsible for these interconversions. When the sample is hydrated, as in MAS NMR measurement, this Al^{III} could appear, at least partially, in a pentacoordinated (except for β zeolite) or octahedral configuration.

Conclusions

The chemical state of aluminum in β zeolite has been established by decomposition of the Al KLL Auger transition. By using an appropriate standard sample for the determination of the full width at half-maximum, three kinds of aluminum coordination could be suggested: tetrahedral (Al^{IV}), octahedral (Al^{VI}), and tricoordinated Al species. From the decomposition of the Al KLL Auger peak of a calcined β containing only Al^{IV}, it has been found that Al^{IV} transforms to Al^{III} and Al^{VI}, with the emergence of Al^{III} being faster than that of Al^{VI}. The change of Al^{III} to Al^{IV} occurring upon ammonium exchange confirmed the reversibility of Al in β zeolites observed by ^{27}Al MAS NMR spectroscopy.

Acknowledgment. F.C. gratefully acknowledges FRIA (Fonds pour la Formation à la Recherche dans l'Industrie et l'Agriculture), Belgium, for a doctoral grant. We are indebted to B. Wouters (Centrum voor Oppervlaktechemie en Katalyse, Leuven, Belgium) for the ^{27}Al MAS-NMR analysis of sample ZB25, and to M. Genet (Unité de Chimie des Interfaces, Louvain-la-Neuve) for useful discussion.

References and Notes

(1) Bourgeat-Lami, E.; Massiani, P.; Di Renzo, F.; Espiau, P.; Fajula, F. *Appl. Catal. A: Gen.* **1991**, *72*, 139.
(2) Bourgeat-Lami, E.; Massiani, P.; Di Renzo, F.; Fajula, F.; Des Courières, T. *Catal. Lett.* **1990**, *5*, 265.
(3) Beck, L. W.; Haw, J. F. *J. Phys. Chem.* **1996**, *99*, 1076.
(4) de Ménorval, L. C.; Buckermann, W.; Figueras, F.; Fajula, F. *J. Phys. Chem.* **1996**, *100*, 465.
(5) Wouters, B.; Chen, T.; Grobet, P. *J. Am. Chem. Soc.* **1954**, *76*, 3129.
(6) Kiricsi, I.; Flego, C.; Pazzuconi, G.; Parker, Jr., W. O.; Millini, R.; Perego, C.;Bellussi, G. *J. Phys. Chem.* **1994**, *98*, 4627.
(7) Jia, C.; Massiani, P.; Barthomeuf, D. *J. Chem. Soc., Faraday Trans.* **1993**, *89*, 3659.
(8) Maache, M.; Janin, A.; Lavalley, J. C.; Joly, J.-F.; Benazzi, E. *Zeolites* **1993**, *13*, 419.
(9) Guisnet, M.; Ayrault, P.; Coutanceau, C.; Fernanda Alvarez, M.; Datka, J. *J. Chem. Soc., Faraday Trans.* **1997**, *99*, 1661.
(10) Loeffler, E.; Lohse, U.; Peuker, Ch.; Oelhmann, G.; Kustov, L. M.; Zholobenko, V. L.; Kazansky, V. B. *Zeolites* **1990**, *10*, 266.
(11) Vimont, A.; Thibault-Staryk, F.; Lavalley, J. C. *J. Phys. Chem. B* **2000**, *104*, 286.
(12) Remy, M.; Genet, M.; Notté, P.; Lardinois, P. F.; Poncelet, G. *Microporous Mater.* **1993**, *2*, 7.
(13) Remy, M.; Genet, M.; Poncelet, G.; Lardinois, P. F.; Notté, P. P. *J. Phys. Chem.* **1992**, *96*, 2614.
(14) Fajula, F.; Bourgeat-Lami, E.; Zivkov, C.; Des Courières, T.; Anglerot, D. Fr. Patent 2,069,618, 1992.
(15) Borade, R. B.; Clearfield, A. *Microporous Mater.* **1996**, *5*, 289.
(16) de Boer, J. H.; Linsen, B. G.; Osinga, T. J. *J. Catal.* **1964**, *4*, 643.
(17) Rouxhet, P.; Genet, M. J. In *Microbial Cell Surface Analysis*; VHC Publishers: New York, 1991; p 206.
(18) Wagner, C. D.; Davis, L. E.; Zeller, M. V.; Taylor, J. A.; Raymond, R. H.; Gale, L. H. *Surf. Interface Anal.* **1981**, *3*, 211.
(19) Coutanceau, C.; Da Silva, J. M.; Alvarez, M. F.; Ribero, F. R.; Guisnet, M. *J. Chim. Phys.* **1997**, *94*, 765.
(20) Szasman, J.; Lieselang, J.; Jenkin, J. G.; Leckey, C. G. *J. Electron Spectrosc.* **1981**, *23*, 37.
(21) Borade, R. B.; Clearfield, A. *J. Phys. Chem.* **1992**, *96*, 6729.
(22) Vaudry, F.; Di Renzo, F.; Fajula, F.; Schulz, P. In *Studies in Surface Science and Catalysis*; Elsevier: Amsterdam, 1994; Vol. 84, p 163.
(23) Stöcker, M. *Microporous Mater.* **1996**, *6*, 235.
(24) West, R. H.; Castle, J. E. *Surf. Interface Anal.* **1982**, *4*, 68.
(25) Barr, T.; Seal, S.; Wozniak, K.; Klinowski, J. *J. Chem. Soc., Faraday Trans.* **1997**, *93*, 181.
(26) Collignon, F.; Poncelet, G. *J. Catal.*, in press.